

A Generalized Stochastic Hydrometeorological Model for Flood and Flash-Flood Forecasting

1. Formulation

KONSTANTINE P. GEORGAKAKOS

Department of Civil and Environmental Engineering and Iowa Institute of Hydraulic Research, The University of Iowa, Iowa City

An attempt to couple meteorological and hydrological models and procedures within the real-time flood forecasting framework is made. A local quantitative precipitation model is coupled to a soil model and a channel routing model through mass conservation differential equations and an automatic updating procedure. Automatic updating is performed through the use of the Extended Kalman Filter that provides the capability for real-time probabilistic forecasts of flood occurrence and flood magnitude. To complement the coupled system, a methodology was developed for consistent spatial interpolation of sparse observations of the pertinent meteorological input variables. The interpolation methodology takes into account topographic relief and atmospheric lapse rates. The result of the modeling effort is a stochastic-dynamic hydrometeorological system suitable for use in real-time flood and flash-flood forecasting.

INTRODUCTION

It has been common practice among hydrologists involved in real-time forecasting of floods to develop rainfall-runoff models that simulate soil and channel processes and utilize precipitation rates as input. The lack of reliable and flexible precipitation models suitable for the spatial and temporal scales of the hydrologic processes (see review by *Georgakakos and Hudlow [1984]*) has prevented the formulation of generalized models that simulated precipitation, soil, and channel processes. Recently, however, *Georgakakos and Bras [1984a, b]* presented a physically based conceptual precipitation model whose tests have given encouraging results. It is the purpose of this paper to present a generalized hydro-meteorological model which couples storm, soil, and channel states in an extended state vector to produce, as an output, flow rates at the drainage basin outlet. The soil moisture accounting portion of the Sacramento model is utilized as the soil response simulator. The precipitation model of *Georgakakos and Bras [1984a]* and the channel routing model of *Georgakakos and Bras [1982b]* are used to provide the input and to propagate downstream the output of the soil model, respectively. The model is suitable for use in operational river flow forecasting since (1) it uses as input operationally forecast surface temperature T_0 , surface pressure p_0 , surface dew-point temperature T_s , and mean areal evapotranspiration potential rate u_e , and (2) it is in state-space form, thus suitable to be used with modern estimation theory techniques which have proven to be of great value in the real-time forecasting of river flows [e.g., *Bras and Rodriguez-Iturbe, 1985; Kitanidis and Bras, 1980a, b; Georgakakos and Bras, 1982b, 1984a, b*].

Some of the characteristics of the stochastic hydro-meteorological model that make it particularly useful in real-time flood forecasting are (1) extended forecast lead time, especially in cases of flash-floods, because of the quantitative precipitation forecast capability; (2) better distribution of the precipitation volume in the various soil zones because of the existence of a dynamic equation for the precipitation state; (3)

improved modeling of uncertainty through the incorporation of a precipitation state in the state vector; and (4) capability for updating the upper soil states from only precipitation observations.

The long distances (order of 100 km) between points where the meteorological input (T_0, p_0, T_d) is forecast (or observed) in real time necessitates an interpolation procedure characteristic of the basin of interest for the determination of T_0, p_0 , and T_d . This paper presents such an interpolation procedure that explicitly takes into account topography and the prevailing lapse rate of the atmosphere (dry adiabatic or pseudoadiabatic). Verification of the interpolation procedure is done using real-world data. In an accompanying paper [*Georgakakos, this issue*], the model is verified using six-hourly hydro-meteorological data from the Bird Creek basin in Oklahoma.

MODEL FORMULATION

Based on the current local moisture content of the atmosphere, soil, and channel, and on forecasts of the meteorological variables T_0, T_d, p_0 , and u_e , the generalized rainfall-runoff model equations are capable of producing rainfall and runoff forecasts for the basin of interest.

The model equations are presented here in a general form for a headwater basin (with no upstream inflows). *Georgakakos and Bras [1982a]*, *Georgakakos [1983]*, and *Puente Angulo and Bras [1984]* extend the formulation to include large-river systems with several tributary basins:

$$\frac{d(x_p)}{dt} = f_p(x_p, \mathbf{u}; \mathbf{a}_p) \quad (1)$$

$$\frac{d(\mathbf{x}_s)}{dt} = \mathbf{f}_s(x_p, \mathbf{x}_s, \mathbf{u}, u_e; \mathbf{a}_p, \mathbf{a}_s) \quad (2)$$

$$\frac{d(\mathbf{x}_c)}{dt} = \mathbf{f}_c(x_p, \mathbf{x}_s, \mathbf{x}_c, \mathbf{u}, u_e; \mathbf{a}_p, \mathbf{a}_s, \mathbf{a}_c) \quad (3)$$

The concurrent precipitation and basin outlet discharge rates are the instantaneous model output variables, given by

$$z_p = h_p(x_p, \mathbf{u}; \mathbf{a}_p) \quad (4)$$

$$z_c = h_c(\mathbf{x}_c; \mathbf{a}_c) \quad (5)$$

Copyright 1986 by the American Geophysical Union.

Paper number 6W4389.
0043-1397/86/006W-4389\$05.00

The notation employed in the previous equations is defined in Appendix A.

Current observation networks give measurements of the instantaneous discharge rate z_c . However, the accumulated precipitation volume z_p^V over a time interval Δt is sampled instead of the instantaneous rate z_p . Equation (4) is utilized with the instantaneous rate z_p related to the volume z_p^V by

$$z_p = z_p^V \Delta t \tag{6}$$

Equations (4) and (5) are valid for discrete time $t, t + \Delta t, t + 2\Delta t, \dots, t + k\Delta t, \dots$.

The functions $f_p, f_s, f_c, h_p,$ and h_c and the parameters $a_p, a_s,$ and a_c are defined in the following sections for the particular cases of the *Georgakakos and Bras* [1984a] precipitation model, the Sacramento soil moisture accounting model [Bur-nash et al., 1973], and the *Georgakakos and Bras* [1982b] channel-routing model.

PRECIPITATION MODEL

The precipitation model of *Georgakakos and Bras* [1984a, b] is based on the conservation of condensed water equivalent mass (model state) in a cloud column characterized by the input variables $T_0, p_0,$ and T_d . Cloud microphysics gives expressions for the precipitation rate as a function of the input variables, the model state, and the storm invariant parameters. Pseudoadiabatic condensation gives the input rate in the cloud column. Although the model formulation has been presented in the work by *Georgakakos and Bras* [1984a], we present the model equations below in order to establish notation and for easy reference. Following the notation of Appen-dixes A and B, the model equations are

$$f_p(x_p, \mathbf{u}; \mathbf{a}_p) = f(\mathbf{u}) - h(\mathbf{u}) \cdot x_p \tag{7}$$

where

$$f(\mathbf{u}) = [w_0 - w_s(T_s, p_s)] \cdot \rho_m \cdot v \tag{8}$$

$$\rho_m = (p_s/R T_s + p_l/R T_l)/2 \tag{9}$$

$$w_0 = w_s(T_d, p_0) \tag{10}$$

$$w_s(T, p) = \varepsilon A_1 \frac{(T - 223.15)^{3.5}}{p} \tag{11}$$

$$v = \varepsilon_1 [c_p(T_m - T_s')]^{1/2} \tag{12}$$

$$p_s = \left(\frac{1}{\frac{T_0 - T_d}{223.15} + 1} \right)^{3.5} p_0 \tag{13}$$

$$T_s = \left(\frac{1}{\frac{T_0 - T_d}{223.15} + 1} \right) T_0 \tag{14}$$

$$T_s' = \frac{T_0}{p_0^{0.286}} (p')^{0.286} \tag{15}$$

$$p' = \frac{3}{4} p_s + \frac{1}{4} p_l \tag{16}$$

The temperature T_m and the pressure p_l are found as the solutions of the system of algebraic equations:

$$T_m \left(\frac{p_n}{p'} \right)^{0.286} \exp \left\{ \frac{L(T_m)w_s(T_m, p')}{c_p T_m} \right\} = \Theta_e \tag{17}$$

$$p_l = p_l + \frac{\varepsilon_2 - p_l}{1 + \varepsilon_3 \varepsilon_1 (c_p (T_m - T_s'))^{1/2}} \tag{18}$$

with

$$\Theta_e = T_s \left(\frac{p_n}{p_s} \right)^{0.286} \exp \left\{ \frac{L(T_s)w_s(T_s, p_s)}{c_p T_s} \right\} \tag{19}$$

$$L(T) = A - B(T - 273.15) \tag{20}$$

The temperature T_l is found as the solution of the algebraic equation,

$$T_l \left(\frac{p_n}{p_l} \right)^{0.286} \exp \left\{ \frac{L(T_l)w_s(T_l, p_l)}{c_p T_l} \right\} = \Theta_e \tag{21}$$

The function $h(\mathbf{u})$ in (7) is given by

$$h(\mathbf{u}) = \frac{V_p}{Z_c \delta} \left[\frac{1 + \frac{3}{4} N_v + \frac{N_v^2}{4} + \frac{N_v^3}{24}}{e^{N_v}} + \frac{1 + \frac{3}{4} (\gamma N_v) + \frac{(\gamma N_v)^2}{4} + \frac{(\gamma N_v)^3}{24}}{\gamma^3 e^{\gamma N_v}} + \frac{N_v}{4\gamma^4} + \frac{1}{\gamma^5} \right] \tag{22}$$

$$V_p = 4\alpha \varepsilon_4 v^m \tag{23}$$

$$N_v = \frac{\beta v^{(1-m)}}{\alpha \varepsilon_4} \tag{24}$$

$$\delta = \frac{1}{3} \left(\frac{1}{\gamma} + \frac{1}{\gamma^2} + \frac{1}{\gamma^3} \right) \tag{25}$$

$$Z_c = \frac{R(T_s + T_l)}{2g} \ln \left(\frac{p_s}{p_l} \right) \tag{26}$$

The observation function $h_p(x_p, \mathbf{u}; \mathbf{a}_p)$ is given by

$$h_p(x_p, \mathbf{u}; \mathbf{a}_p) = \phi(\mathbf{u}) \cdot x_p \tag{27}$$

where

$$\phi(\mathbf{u}) = \frac{V_p}{Z_c \delta} \left[\zeta \left(\frac{N_D}{N_v} \right) \frac{\left(1 - \frac{N_v}{4} \right) \left(1 + N_D + \frac{N_D^2}{2} \right) + \frac{N_D^3}{8}}{e^{N_D}} + \left(1 - \zeta \left(\frac{N_D}{N_v} \right) \right) \frac{1 + \frac{3}{4} N_v + \frac{1}{4} N_v^2 + \frac{1}{24} N_v^3 - \frac{1}{24} N_D^3}{e^{N_v}} \right] \tag{28}$$

$$\zeta(y) = 1 \quad \text{if } y \geq 1 \tag{29}$$

$$\zeta(y) = 0 \quad \text{if } y < 1$$

$$N_D = \frac{D_c}{\varepsilon_4 v^m} \tag{30}$$

$$D_c = \left[\frac{1}{c_1} \frac{4D_{AB}}{R_c} Z_b \left(\frac{e_s(T_w)}{T_w} - \frac{e_s(T_d)}{T_0} \right) \right]^{1.3} \tag{31}$$

$$e_s(T) = A_1 (T - 223.15)^{3.5} \tag{32}$$

$$Z_b = \frac{R(T_s + T_0)}{2g} \ln \left(\frac{p_0}{p_s} \right) \tag{33}$$

The temperature T_w is the solution of the algebraic equation,

$$T_w = T_0 - \frac{L(T_0)}{c_p} [w_s(T_w, p_0) - w_s(T_d, p_0)] \tag{34}$$

The diffusivity of water vapor in air varies with temperature T_0 and pressure p_0 according to

$$D_{AB} = A_2 \left(\frac{T_0}{T^*} \right)^{1.94} \left(\frac{p^*}{p_0} \right) \tag{35}$$

TABLE 1. Soil Moisture Accounting Model Variables

Symbol	Description	Value
<i>States (Vector x_s)</i>		
x_1	upper zone tension water content, mm	
x_2	upper zone free water content, mm	
x_3	lower zone tension water content, mm	
x_4	lower zone primary free water content, mm	
x_5	lower zone secondary free water content, mm	
x_6	additional impervious storage, mm	
<i>Inputs</i>		
u_e	instantaneous evapotranspiration demand, mm/6 hours	
P_v	instantaneous precipitation input, mm/6 hours	
<i>Parameters (Vector a_s)</i>		
x_1^0	upper zone tension water capacity, mm	120
x_2^0	upper zone free water capacity, mm	15
x_3^0	lower zone tension water capacity, mm	160
x_4^0	lower zone primary free water capacity, mm	140
x_5^0	lower zone secondary free water capacity, mm	14
d_u	upper zone instantaneous drainage coefficient, 1/6 hours	0.089
d_i'	lower zone primary instantaneous drainage coefficient, 1/6 hours	0.003
d_i''	lower zone secondary instantaneous drainage coefficient, 1/6 hours	0.033
ϵ	parameter in percolation function	48
θ	exponent in percolation function	2.1
P_f	fraction of percolated water assigned to the lower zone free water aquifers	0.02
μ	fraction of base flow not appearing in river flow	3.55
β_1	fraction of basin that becomes impervious when tension water requirements are met	0.17
β_2	fraction of basin permanently impervious	0.001
m_1	exponent of the upper zone tension water nonlinear reservoir	2
m_2	exponent of the upper zone free water nonlinear reservoir	2
m_3	exponent of the lower zone tension water nonlinear reservoir	2

Appendix B gives the constants, input variables, and model parameters of the precipitation model presented.

The values of the model parameters are based on the work of Georgakakos and Bras [1984b] and Georgakakos [1982, 1984]. Their results indicate that the 'optimal' parameter values remain reasonably constant for various storm types, various topographic locations, and various optimization criteria.

SOIL MOISTURE ACCOUNTING MODEL

The soil moisture accounting scheme of the National Weather Service River Forecast System (NWSRES) has been successfully used with modern estimation theory techniques for the real-time forecasting of river flows [Kitanidis and Bras, 1980a, b; Georgakakos and Bras, 1979; Georgakakos and Bras, 1982b; Restrepo-Posada and Bras, 1982]. It is a conceptual model of the reservoir type that monitors the volume of water in the various soil layers. Description of the deterministic model is given in Burnash et al. [1973] and in the work by Peck [1976]. Armstrong [1978] gives the physical interpretation of the model components in terms of the observable soil characteristics. The differential equations for the time evolution of the model states, which are the contents of each con-

ceptual reservoir, have been formulated in the work by Kitanidis and Bras [1980a].

Previous formulations characteristically represent outflow from a certain conceptual reservoir as a discontinuous function of its contents. For instance, the upper zone tension water reservoir, modeling upper soil layer and interception storage, produces zero outflow until its contents equal its capacity. Once the reservoir is full its output is equal to its net input. This type of behavior is very difficult to handle within the linear framework of the most powerful modern estimation techniques. Kitanidis and Bras [1980a], in their formulation of the linearized system, use describing function techniques to avoid the problem.

This work substitutes the threshold-type behavior of the reservoir outflow (wherever applicable in the model) with a nonlinear reservoir response. This way the reservoir produces outflow even if it is not full, and its outflow depends on the degree of saturation. From a physical point of view, this is consistent with the spatially lumped nature of the model, given the inhomogeneity of the soil properties of the basin. Thus even if each soil column behaves as a threshold-type reservoir, the basin produces continuous outflow to groundwater and to the channel because of the spatial variation of the threshold value. In this work, the model parameter that defines the threshold (reservoir capacity) is considered to be a basinwide maximum capacity of the soil columns.

Apart from the removal of the discontinuities, the following were important model modifications. The moisture input to the soil moisture accounting scheme is taken from

$$P_v = \phi x_p \tag{36}$$

with P_v the volume rate per unit area and x_p the volume in cloud storage. The dependence of ϕ on u has been omitted for notational convenience.

The distribution function for allocation of the percolating water between the lower zone free water reservoirs has been replaced by a numerically better behaving one. Use of the function in the original NWS model within a state estimation algorithm is liable to produce incorrect results [Analytic Sciences Corporation, 1980]. The modification is presented in the work by Georgakakos et al. [1980] and the result is

Portion allocated to primary storage

$$\left(C_2 \frac{x_5}{x_5^0} - 1 \right) \frac{x_4}{x_4^0} + 1$$

Portion allocated to secondary storage

$$\left(1 - C_2 \frac{x_5}{x_5^0} \right) \frac{x_4}{x_4^0}$$

with C_2 defined by

$$C_2 = \frac{d_i' x_4^0}{d_i' x_4^0 + d_i'' x_5^0} \tag{37}$$

Table 1 shows the list of symbols used in the soil moisture accounting equations together with their description. It is mostly based on the notation introduced by Analytic Sciences Corporation [1980]. (See also Kitanidis and Bras [1980a]. The parameter values for the Bird Creek Basin are also shown in Table 1. The parameter rate values correspond to a standard interval of 6 hours.

A difference between the present formulation and the one

published in the work by *Kitanidis and Bras* [1980a] is that the equations to follow include the surface runoff outflow from the additional impervious area. In this aspect the present formulation agrees with the one in the work by *Georgakakos et al.* [1980]. Depending on the hydrogeomorphologic characteristics of the basin under study, this component of outflow may or may not be significant.

To facilitate notation, define the quantities y and C_1 as

$$y = 1 - \frac{x_3 + x_4 + x_5}{x_3^0 + x_4^0 + x_5^0} \quad (38)$$

$$C_1 = d_1' x_4^0 + d_1'' x_5^0 \quad (39)$$

If the i th component of the vector function $f_i(\cdot)$ is denoted by f_{s_i} , the applicable differential equations are as follows.

Upper zone tension water element

$$f_{s_1} = \left[1 - \left(\frac{x_1}{x_1^0} \right)^{m_1} \right] \phi x_p - u_e \frac{x_1}{x_1^0} \quad (40)$$

Upper zone free water element

$$f_{s_2} = \left(\frac{x_1}{x_1^0} \right)^{m_1} \phi x_p \left[1 - \left(\frac{x_2}{x_2^0} \right)^{m_2} \right] - d_u x_2 - C_1 (1 + \varepsilon y^\theta) \frac{x_2}{x_2^0} \quad (41)$$

Lower zone tension water element

$$f_{s_3} = C_1 (1 + \varepsilon y^\theta) \frac{x_2}{x_2^0} (1 - P_f) \left[1 - \left(\frac{x_3}{x_3^0} \right)^{m_3} \right] - u_e \left(1 - \frac{x_1}{x_1^0} \right) \frac{x_3}{x_1^0 + x_3^0} \quad (42)$$

Lower zone primary free water element

$$f_{s_4} = -d_1' x_4 + C_1 (1 + \varepsilon y^\theta) \frac{x_2}{x_2^0} \left[1 - (1 - P_f) \left[1 - \left(\frac{x_3}{x_3^0} \right)^{m_3} \right] \right] \cdot \left[\left(C_2 \frac{x_5}{x_5^0} - 1 \right) \frac{x_4}{x_4^0} + 1 \right] \quad (43)$$

Lower zone secondary free water element

$$f_{s_5} = -d_1'' x_5 + C_1 (1 + \varepsilon y^\theta) \frac{x_2}{x_2^0} \left[1 - (1 - P_f) \left[1 - \left(\frac{x_3}{x_3^0} \right)^{m_3} \right] \right] \cdot \left(1 - C_2 \frac{x_5}{x_5^0} \right) \frac{x_4}{x_4^0} \quad (44)$$

Additional impervious area water element

$$f_{s_6} = \left[1 - \left(\frac{x_6 - x_1}{x_3^0} \right)^2 \left(\frac{x_1}{x_1^0} \right)^{m_1} \right] \phi x_p - u_e \left(1 - \frac{x_1}{x_1^0} \right) \left(\frac{x_6 - x_1}{x_3^0 + x_1^0} \right) - u_e \frac{x_1}{x_1^0} - \left[1 - \left(\frac{x_6 - x_1}{x_3^0} \right)^2 \right] \left(\frac{x_2}{x_2^0} \right)^{m_2} \left(\frac{x_1}{x_1^0} \right)^{m_1} \phi x_p \quad (45)$$

The output u_c from the soil moisture accounting model, referred to as total channel inflow per unit time, is given by

$$u_c = \left(d_u x_2 + \frac{d_1' x_4 + d_1'' x_5}{1 + \mu} \right) (1 - \beta_1 - \beta_2) + \phi x_p \beta_2 + \left(\frac{x_6 - x_1}{x_3^0} \right)^2 \phi x_p \left(\frac{x_1}{x_1^0} \right)^{m_1} \beta_1$$

$$+ \phi x_p \left(\frac{x_1}{x_1^0} \right)^{m_1} \left(\frac{x_2}{x_2^0} \right)^{m_2} (1 - \beta_1 - \beta_2) + \left[1 - \left(\frac{x_6 - x_1}{x_3^0} \right)^2 \right] \left(\frac{x_2}{x_2^0} \right)^{m_2} \left(\frac{x_1}{x_1^0} \right)^{m_1} \phi x_p \beta_1 \quad (46)$$

The following constraints determine the definition domain of the state variables x_i^0 :

$$0 \leq x_i \leq x_i^0 \quad i = 1, 2, \dots, 5 \quad (47)$$

It should be noted that (40) and (41) are mathematical approximations in that the nonlinear reservoir outflow does not depend on the current net input, but rather on the nonnegative portion of it. This may result, for example, in a situation where the filled upper zone tension water element will be depleted by evapotranspiration even though the current precipitation rate might be greater than the actual evapotranspiration rate. Given, however, the small time increments in which the integration of the differential equations will proceed, the error introduced will be well within the overall model structure errors.

CHANNEL-ROUTING MODEL

Georgakakos and Bras [1980, 1982b] presented a conceptual, nonlinear, reservoir-type channel routing model, which when tested with the soil moisture accounting scheme of the NWSRFS, showed improved performance over linear black box type models. Their model is simple to implement on a digital computer and it does not require a large quantity of high quality input data, as do the routing models based on the full momentum and continuity equations.

The idea is to represent the channel as a cascade of n reservoirs. Let $S_i(t)$ be the volume of water in storage at the i th reservoir and $u_c(t)$ the total channel inflow per unit time (for example, the output of the soil moisture accounting scheme presented previously).

Then denoting by f_{c_i} the i th component of f_c , the model differential equations for a headwater basin with no upstream inflows, are

$$f_{c_i} = p_i u_c(t) + a_{i-1} S_{i-1}^m(t) - a_i S_i^m(t) \quad (48) \\ i = 1, 2, \dots, n \quad a_0 = 0$$

and the instantaneous discharge rate at the basin outlet is given by

$$h_c(x_c; a_c) = a_n S_n^m(t) \quad (49)$$

The i th component of the channel state vector x_c is S_i . Parameters of the model are p_i , a_i , ($i = 1, 2, \dots, n$), m , and n . *Georgakakos and Bras* [1980] give the details of model formulation as well as ways of estimating model parameters from (1) the basin observable hydromorphologic characteristics and (2) input-output time series data.

The table below gives the values of the model parameters (vector a_c) for the Bird Creek basin.

Channel Model Parameters

$n = 3$
$m = 0.8$
$a_1 = 1.09$ (mm ^{0.2} , 6 hours)
$a_2 = 1.04$ (mm ^{0.2} , 6 hours)
$a_3 = 1.08$ (mm ^{0.2} , 6 hours)

STATE ESTIMATOR

Statistical filters will effectively couple the state variables of the soil and channel models with those of the precipitation

model. This is a different coupling than the one due to the conservation of water-mass law. The effect that each state variable has on the storm basin model output variables is monitored through the filter equations. Each state variable is updated from the system observations, based on the degree of its correlation to the model output variables and to the rest of the model variables. In this way the errors in predicting the discharge at the catchment outlet have a bearing on the specification of the initial conditions of the precipitation model variables. Similarly, observations of the precipitation state variables and parameters have an effect on the determination of the state variables related to the drainage basin. This assures coordination in the operation of the coupled storm and basin models in real time.

Use of a state estimator with the hydrometeorological model offers the capability of probabilistic forecasts. Based on the predicted mean state vector and the predicted covariance matrix, one can obtain the mean and the variance of the predicted observation variables. Then, assuming a normal distribution for the prediction errors, and given a critical flood flow threshold, one can compute the probability of the threshold exceedance and, therefore, the probability of flooding. This probability value is indispensable in present day decision-making processes.

Georgakakos and Bras [1982a] develop the formulation of the stochastic hydrometeorological model in a linear statistical filter framework. Their formulation allows for uncertain input with given mean and variance. Since the system equations (i.e., equations (1) through (5)) are nonlinear, both in the system states and the input, the extended Kalman filter is used as the state estimator [Gelb, 1974]. The procedure is straightforward to implement and the interested reader is referred to Georgakakos and Bras [1982a] [also Bras and Rodriguez-Iturbe, 1985] for the details. It should be noted, however, that the stochastic formulation introduces new parameters related to the filter covariance equations. These are the elements of the system noise covariance parameter matrix Q and the elements of the observation noise covariance matrix R .

METEOROLOGICAL INPUT SPATIAL INTERPOLATION

The Georgakakos and Bras [1984a, b] precipitation model uses surface meteorological data as input in order to forecast the precipitation rate in the area characterized by the input. It is often the case, with the present state of the surface meteorological data network (average distance between stations of the order of 100 km), that the precipitation rate is sought in areas where no observations (or accurate forecasts) of the input exist. Interpolation of surface meteorological observations is then necessary. This section examines the issue of the spatial interpolation of air temperature T_0 , pressure p_0 , and dew point temperature T_d near the ground surface of terrain of varying altitude.

It is assumed that surface meteorological input is determined by both topography and atmospheric disturbances. The input is decomposed into two corresponding parts $u_t(z)$ and u_a , according to

$$u = u_t(z) + u_a \tag{50}$$

where u denotes input (any of T_0 , p_0 , T_d); z denotes altitude; $u_t(z)$ is the altitude-dependent topography component; and u_a is the atmospheric component. The various interpolation strategies for each component are presented in the following sections.

Topographic Component of Input

An air parcel is followed as it is forced by the topographic relief to ascend from the lowest point in the area under consideration. The thermal properties (pressure and temperature) of the parcel are determined from its initial properties at the lowest point and from the assumption of heat-adiabatic ascent in unsaturated environment or pseudoadiabatic ascent in saturated environment. The available equations are [Wallace and Hobbs, 1977] as follows. The hypsometric equation (see also equations (26) and (33)),

$$z - z_l = \frac{RT_{av}}{g} \ln \left(\frac{p_l}{p} \right) \tag{51}$$

The equation for the dry adiabatic lapse rate,

$$(dT/dz)_{dry\ parcel} = -g/c_p \tag{52a}$$

or, given initial condition T_l at altitude z_l ,

$$T = -\frac{g}{c_p} (z - z_l) + T_l \tag{52b}$$

The equation for saturated adiabatic ascent (see also equations (17), (19), and (21)),

$$\theta_e = T \left(\frac{p_a}{p} \right)^{0.286} \exp \left\{ \frac{L(T)w_s(T, p)}{c_p T} \right\} \tag{53}$$

In the above equations the subscript l denotes quantities at the lowest point in the area under consideration. Also, T_{av} is the average temperature in the layer between altitudes z and z_l . All other quantities have been defined in the previous section.

The methodology for the removal of topographic effects is summarized in the following steps.

1. Record the temperature T_{0l} , pressure p_{0l} , and dew-point temperature T_{dl} at the lowest point in the area of interest. Determine the saturation degree of the air based on the inequalities

$$\begin{aligned} T_{0l} > T_{dl} & \quad \text{unsaturated} \\ T_{0l} = T_{dl} & \quad \text{saturated} \end{aligned}$$

2. If $T_{0l} > T_{dl}$, use (52b) to determine the temperature of an air parcel, after its heat-adiabatic ascent, at height z below the lifting condensation level z_L , where the air just becomes saturated. The altitude z_L is defined by (51) when $p = p_s$ and $T_{av} = (T_s + T_{0l})/2$, and with p_s and T_s given by (13) and (14) respectively.

(1) For $z \geq z_L$ the parcel will rise following the pseudoadiabatic that originates at T_s and p_s . Therefore solve (51) and (53) simultaneously for p and T , given z , p_{0l} , T_{0l} , and θ_e (by means of equation (19)). Using the procedure described, one can obtain the topography component of the surface temperature input $T_l(z)$ for all the altitudes z of interest. Then, using

$$T_{av} = (T_{0l} + T_l(z))/2$$

and (51) solved for p ,

$$p = p_{0l} \exp \left\{ -\frac{(z - z_l)g}{T_{av}R} \right\} \tag{54}$$

obtain the topography component in the surface pressure input $p_l(z)$.

(2) For $z \leq z_L$, the dew-point temperature of the ascending parcel is equal to the one at the lowest point; that is,

$$T_{dl}(z) = T_{dl} \quad z \leq z_L \tag{55}$$

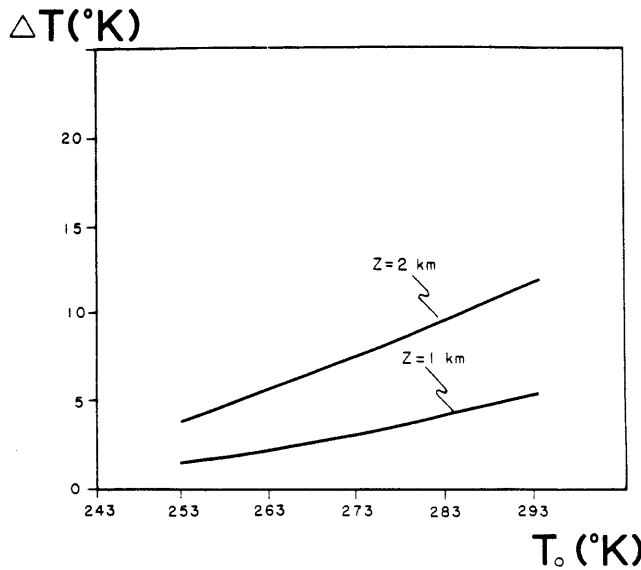


Fig. 1. Difference in temperature between heat-adiabatic and pseudoadiabatic descent from level z to the mean sea level based on the U.S. Standard Atmosphere (computed from the pseudoadiabatic chart in the work by Wallace and Hobbs [1978]).

For parcel ascent above z_L , the air is saturated; therefore

$$T_d(z) = T_i(z) \quad z \geq z_L \quad (56)$$

Since T_d is equal to $T_i(z_L)$, the function $T_d(z)$ is continuous. At this stage, the effects of topography are given through the functions $T_i(z)$, $p_i(z)$, and $T_d(z)$ for all z .

3. If $T_0 = T_d$, then the lifting condensation level is at the lowest point. Proceed as in step (2), case $z \geq z_L$.

The key assumption in the proposed methodology is that there are observations of T_0 , p_0 , and T_d at the lowest point in

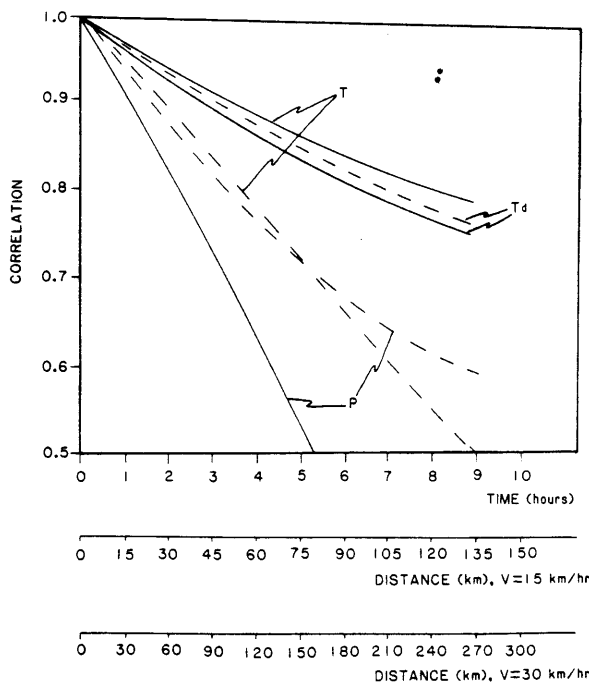


Fig. 2. Time-space correlation functions for T , p , and T_d from Boston, Massachusetts (solid curve) and from Tulsa, Oklahoma (dashed curve) storms. Conversion from time to distance is made based on the constant velocity of the atmospheric disturbance V .

TABLE 2. Topographic Characteristics of Stations Used in the Interpolation Tests

Station	Longitude	Latitude	Altitude, m
Wichita, Kansas	97°25'W	37°39'N	396
Springfield, Missouri	93°23'W	37°14'N	380
Oklahoma City, Oklahoma	97°36'W	35°24'N	384
Tulsa, Oklahoma	95°54'W	36°11'N	200
Billings, Montana	108°32'W	45°48'N	1087
Great Falls, Montana	111°21'W	47°29'N	1116
Lewistown, Montana	109°25'W	46°55'N	1493

the area of interest. In practice, there will be situations where this is not the case. If the points of interest lie above the lowest point where observations are available, the proposed methodology is still applicable. Also for the cases where one is interested in points of lower elevation than the lowest observation station, and the station observations indicate unsaturated conditions ($T_0 > T_d$), then one can use the heat adiabatic descent (52b), together with (51) and (55) to determine the topography components.

Problems arise when the observations indicate saturated conditions at the lowest observation point and points of interest lie on even lower elevations. Because one cannot assess from the available information whether the lifting condensation level is at the observation altitude or lower, one cannot decide whether to use the heat-adiabatic descent or the pseudoadiabatic descent based on some assumption as to the location of the lifting condensation level.

Figure 1 presents the difference in temperature between heat-adiabatic and pseudoadiabatic descent from the lowest observation station to the lowest point in the area of interest as a function of T_0 (the temperature at the level of the initiation of the descent) for 1 and 2 km of total descent. The difference in temperature shown corresponds to the upper bound of the temperature error committed by making any assumption regarding the lapse rate of the atmosphere in the range from adiabatic to pseudoadiabatic. The heat-adiabatic descent corresponds to the situation in which the lifting condensation level is at the same altitude as the lowest observation station. The pseudoadiabatic descent corresponds to the situation in which the lifting condensation level is at the lowest point in the area of interest. It can be seen that the errors made are smaller: the lower the temperature T_0 and the lower the altitude z . Although Figure 1 can serve as a guide to anticipated errors in the case where it is of interest to know the temperature and pressure fields at the bottom of a deep

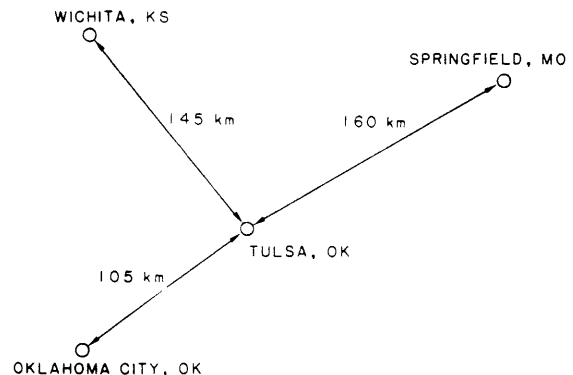


Fig. 3. Plan view of the station configuration with the distances from Tulsa, Oklahoma (kilometers).

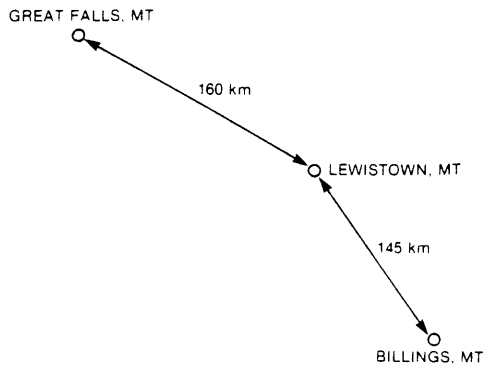


Fig. 4. Plan view of the station configuration with the distances from Lewistown, Montana (kilometers).

valley when the observation stations are at higher altitudes, the occurrence of such a situation in practice is very rare. It is rather the orographic effects that one wants to assess based on observations at low altitudes.

At the expense of increased computational effort, improved accuracy can be obtained if the atmosphere is discretized into several horizontal pressure layers along the vertical direction. Thus one can use several layers to compute $T_i(z)$ and $p_i(z)$ in step 2(1). Increased accuracy is expected mainly because of the nonlinear character of (50), (53), and (54) with respect to temperature and pressure. Because this methodology is intended for use in real-time applications, no vertical discretization was performed for the purposes of this work.

Atmospheric Disturbance Component of Input

Attention is now concentrated on the determination of the component u_a of the meteorological input u for all the points in the area of interest. Suppose that there are N observation stations within reasonable distance (less than 200 km) from the area of interest. First, the field values $T_i(z)$, $p_i(z)$, and $T_{d_i}(z)$ are subtracted from the data of all stations to obtain altitude-equivalent observations. Denote those by T_i , p_i , and T_{d_i} for $i = 1, \dots, N$. The problem now is to optimally interpolate in space the "observations" T_i , p_i , and T_{d_i} .

In applications where the area of interest is of the order of 10,000 (km²) or less, the number N is small. Usually it is less than 10 and very often less than 5. The sparsity of data thus excludes interpolation procedures of the kriging type [e.g., Ripley, 1981]. The assumption of an underlying trend surface defined by a set of parameters to be determined from historical data is not particularly appealing, since the surface thus estimated would be the long term average one rather than the one due to a temporary passage of an atmospheric disturbance. Furthermore, the trend (if one really exists) in ground-based coordinates is a function of the direction of the disturbance movement (e.g., fronts), which is expected to vary among different disturbances.

The previous discussion motivates the use of simple interpolation procedures of the moving average type where the value of T_a or p_a or T_{d_a} (i.e., u_a) at a certain point is a weighted average of the observations T_i , p_i , T_{d_i} , $i = 1, \dots, N$, with weights dependent on distance. Thus weights analogous to D^{-r} , e^{-r} , e^{-rD^2} , with D denoting distance and r a parameter, have been proposed and used with moving average schemes [e.g., Ripley, 1981]. If the weights are denoted by $W(D_i)$, the atmospheric disturbance component u_a at a point in distance D_i from the i th station, $i = 1, \dots, N$, is given by

$$u_a = \sum_{i=1}^N W(D_i)u_i \tag{57}$$

with u_a one of the T_a , p_a , or T_{d_a} and with u_i the corresponding one of the T_i , p_i , or T_{d_i} . Note that the following also holds:

$$\sum_{i=1}^N W(D_i) = 1$$

An indication of the spatial variation of T_a , p_a , and T_{d_a} can be obtained from time series data from a particular station, under the assumption that the disturbances that caused the time series were moving with constant velocity V . Thus using V , one can convert a time correlation to a space correlation.

Figure 2 presents the time-space correlation functions of T , p , and T_d for positive lags, based on data from storms at Boston, Massachusetts (solid curve) and Tulsa, Oklahoma

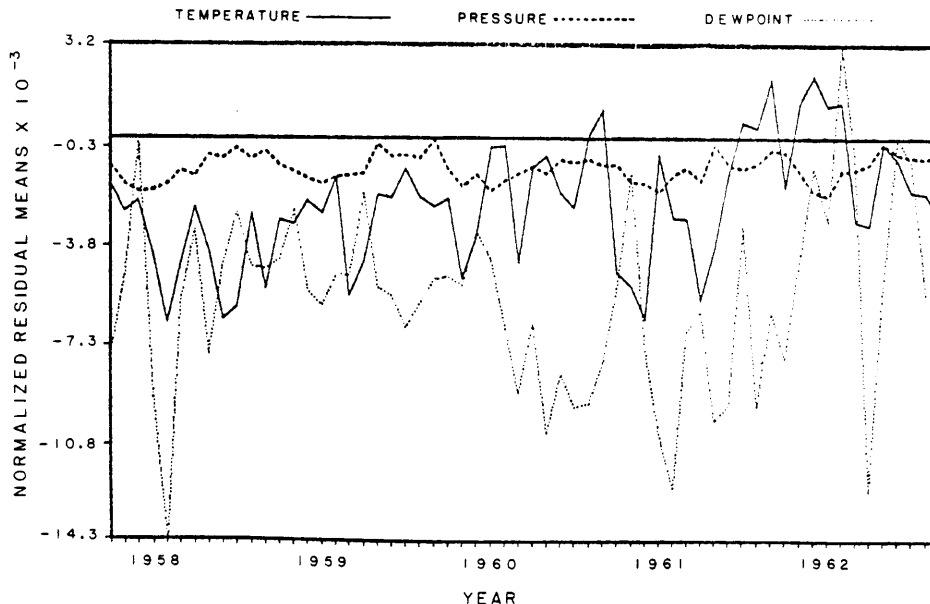


Fig. 5. Residual monthly means normalized by total record observations means for Tulsa, Oklahoma. Only the topography component was used as an estimator.

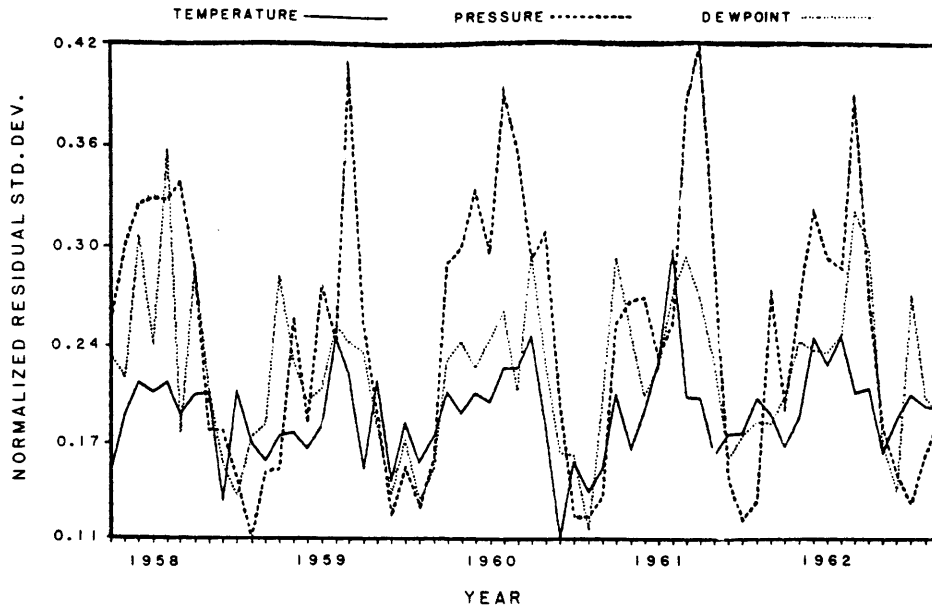


Fig. 6. Residual monthly standard deviations normalized by total record observations standard deviations for Tulsa, Oklahoma. Only the topography component was used as an estimator.

(dashed curve). A total of 300 data values, all from storm periods, were used in each case. The upper horizontal axis is in units of time (hours), while the two lower ones are in units of distance (kilometers) based on velocities of 15 km/hour (top) and 30 km/hour (bottom). Figure 2 indicates linear dependence for all variables at distances up to 100 km. Therefore it is reasonable to use weights that are inversely proportional to distance.

Once the component u_a has been determined for the points of interest, the input u is determined based on (50). It is u that is used as an input to the precipitation model of *Georgakakos and Bras* [1984a, b].

REAL-WORLD APPLICATIONS OF THE INPUT INTERPOLATION PROCEDURE

The interpolation methodology is demonstrated by way of application at the Tulsa, Oklahoma, and at the Lewistown, Montana, areas. Six-hourly temperature, pressure, and dewpoint data were used in both cases. Data from Wichita (Kansas), Springfield (Missouri), and Oklahoma City (Oklahoma) were utilized to determine the meteorological variables at Tulsa (Oklahoma). Data from Billings (Montana) and Great Falls (Montana) were utilized for Lewistown (Montana).

The longitude, latitude, and elevation of all stations are

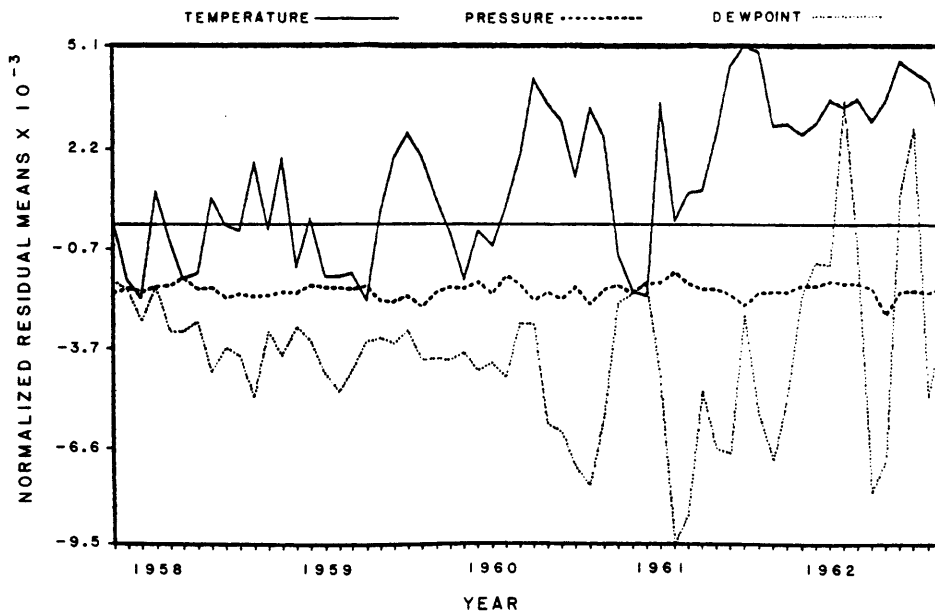


Fig. 7. Residual monthly means normalized by total record observations means for Tulsa, Oklahoma. Both the topography component and the atmospheric disturbances component were used in the interpolation.

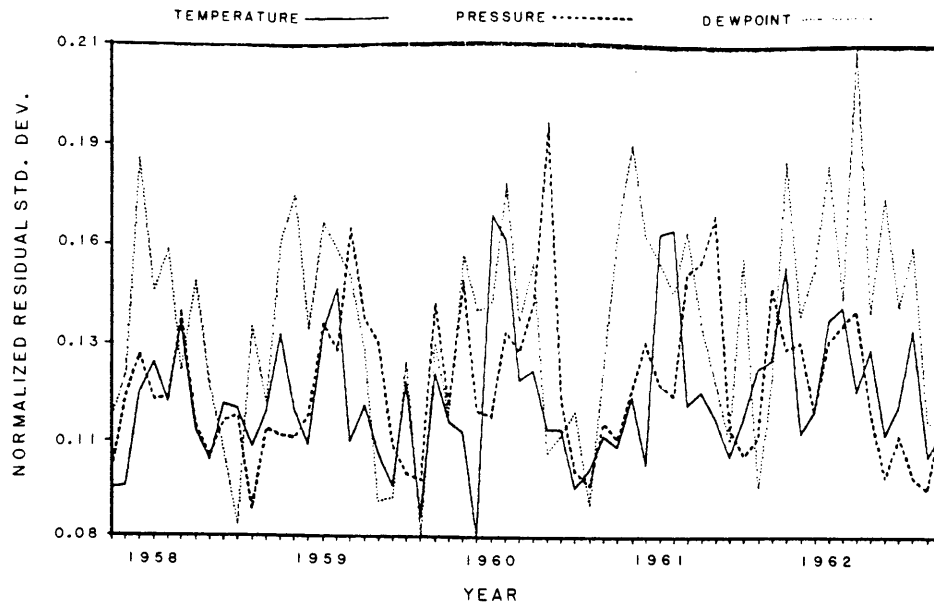


Fig. 8. Residual monthly standard deviations normalized by total record observations standard deviations for Tulsa, Oklahoma. Both the topography component and the atmospheric disturbances component were used in the interpolation.

given in Table 2. Figures 3 and 4 give the relative positions of the stations on a horizontal plane with the interstation distances indicated. The difference in the two test cases lies in the different topographic and climatic regimes. The Oklahoma case is characterized by a flat topographic regime at low elevations with an average air temperature of 15°C. The Montana case is characterized by pronounced topographic relief with cold temperatures averaging 5°C throughout the year. (Temperatures lower than -40°C occur in January and February.) The interstation distances are about the same in the two cases under study.

Tulsa, Oklahoma Case

In this case the elevation of the point of interest (Tulsa) is lower than the elevation of all the other stations. Based on the previous discussion of the interpolation algorithm, performance is expected to be better in other cases, when interest is on the orographic effects at high elevations.

A total of 5 years of 6-hourly data were processed. First, the meteorological quantities attributable to topography at Tulsa were obtained and compared to the corresponding observations [component $u_i(z)$] there (Figures 5 and 6). Then, the full interpolation algorithm was used to obtain the Tulsa quantities and the residual errors were obtained (Figures 7 and 8). The results are summarized in averages over every month of record. The figures present normalized quantities so that performance of the algorithm with respect to different quantities can be compared. Figures 5 and 7 present plots of the residual monthly means normalized by means of the total record observations (at Tulsa). Figures 6 and 8 present plots of the residual monthly standard deviations normalized by the stan-

dard deviations of the total record observations (at Tulsa). Table 3 presents the total record statistics for all meteorological quantities. Comparison of Figures 5 and 6 to Figures 7 and 8 shows that although the topography component explained a large portion of the variance in all quantities, the weighted average interpolation reduced by about one-half the scale of the residual variability due to the topography component alone while giving more "unbiased" estimates. In terms of the various meteorological variables, Figure 7 suggests that the dew-point temperature had the consistently larger negative bias (underestimated) and the air temperature had the highest positive bias (overestimated). Thus the interpolation methodology characterized the atmosphere as being drier than it really was. Variations in the standard deviation (Figure 8) showed similar scales for all the variables, with apparent annual cycles. Examination of the precipitation record for Tulsa showed that the "lows" in the variations of Figure 8 are in the excessively wet months of the year, that is, in the period from May until August. It is this period that is of interest in real-time flood forecasting. On the average, about 87% of the standard deviation of all quantities has been explained by the procedure suggested.

Table 4 gives the overall residual standard deviations for the interpolation methodology. The standard deviation of the residuals for each one of the meteorological variables can be used as the input error standard deviation in the stochastic hydrometeorological model formulated previously.

Lewistown, Montana. Case

A total of 2 years of 6-hourly data were processed. Figures 9 and 10 present plots of the normalized interpolation residuals

TABLE 3. Total Record Statistics for Tulsa, Oklahoma

Variable	Mean	Standard Deviation
Temperature	287.97, °K	10.60, °K
Pressure	99,283, kg (m/s ²)	691, kg/(m/s ²)
Dew-point temperature	281.62, °K	10.40, °K

TABLE 4. Total Record Residual Standard Deviations for Tulsa, Oklahoma

Variable	Standard Deviation
Temperature	1.1, °K
Pressure	80, kg/(m/s ²)
Dew-point temperature	1.5, °K

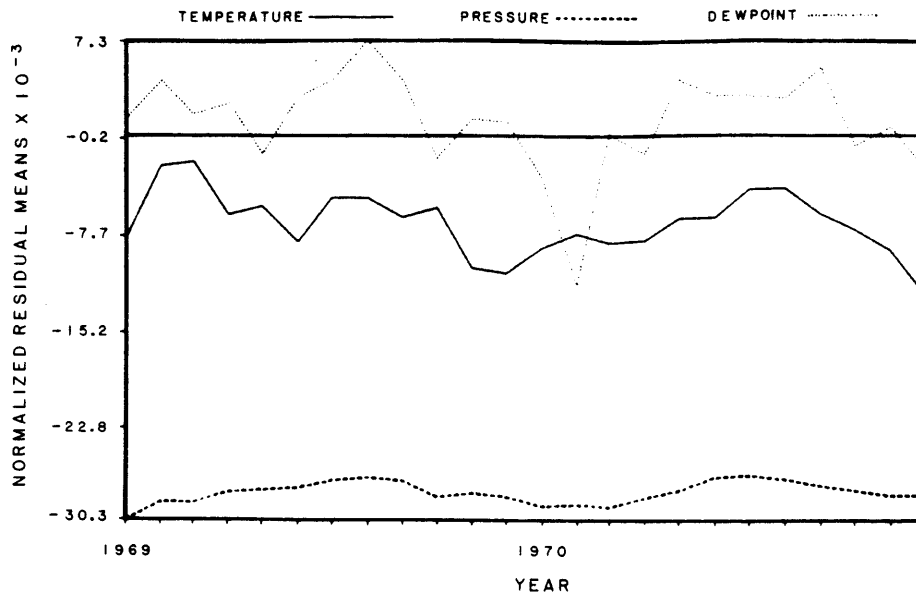


Fig. 9. Residual monthly means normalized by total record observations means for Lewistown, Montana. Only the topography component was used as an estimator.

when the interpolated values were equal to the topography component $u_i(z)$. Figures 11 and 12 correspond to the interpolation residuals when the full interpolation algorithm was used. The total record statistics for temperature, pressure, and dew-point temperature are given in Table 5.

The variance obtained when the topography component alone is used as an estimator is not drastically reduced by the use of the full interpolation algorithm (see Figures 10 and 12). Therefore the topography component explains most of the variance of the observations. Small bias reduction was realized, also, when the full interpolation algorithm was used (see Figures 9 and 11). Figure 11 suggests that the dew point tem-

perature estimates had consistently smaller negative bias (underestimated) than the temperature estimates. Therefore in this case the interpolation methodology characterized the atmosphere as being moister than it really was.

Variations in the standard deviation (Figure 12) showed similar scales for all the variables with pronounced errors in the cold months December and January. The errors in those months are to a large extent due to large estimation errors in the saturation vapor pressure $e_s(T)$ (see also equation (11)):

$$e_s(T) = A_1(T - 223.15)^{3.5}$$

The formula adopted is a reasonable approximation [see

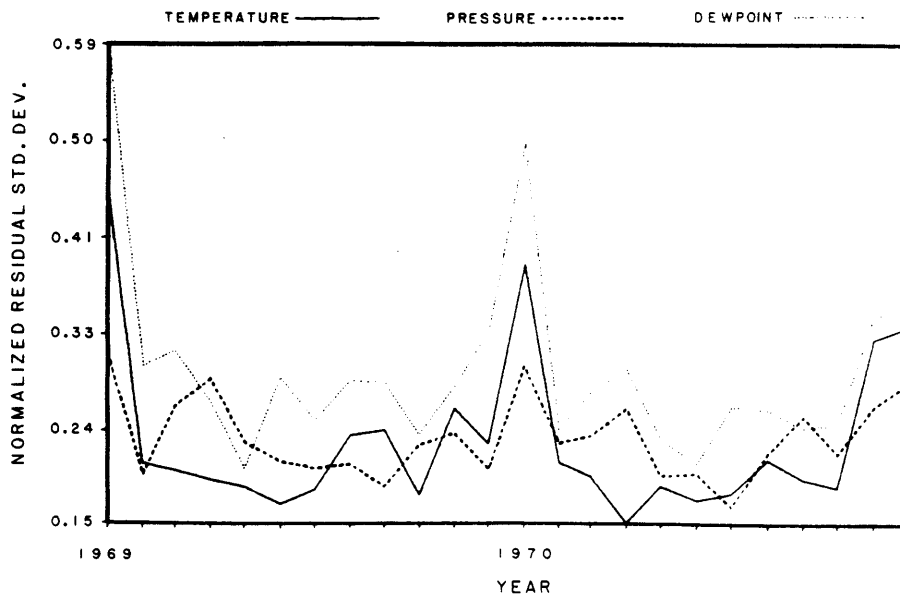


Fig. 10. Residual monthly standard deviations normalized by total record observations standard deviations for Lewistown, Montana. Only the topography component was used as an estimator.

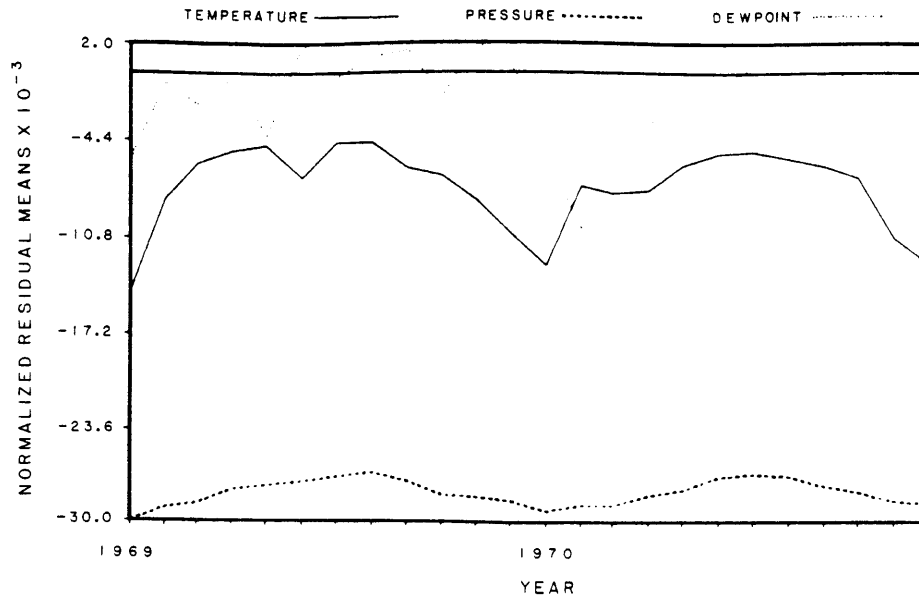


Fig. 11. Residual monthly means normalized by total record observations means for Lewistown, Montana. Both the topography component and the atmospheric disturbances component were used in the interpolation.

Georgakakos and Bras, 1984a] of the saturation vapor pressure over the range of temperature from -30°C (243.15°K) to $+30^{\circ}\text{C}$ (305.15°K). In December and January temperatures lower than -30°C are often recorded at all stations. Therefore errors in the computation of the topography component may result. Note that the Lewistown case is an extreme case in that respect. Certainly, in cases when the algorithm is used to provide input to a hydrometeorological model, much higher temperatures are expected.

Table 6 gives the overall residual standard deviations for the interpolation methodology. In this case too, the values of Table 6 remained constant when weighting functions of distance other than the $(1/\text{distance})$ ones (used in Figures 11 and 12) were utilized.

Comparison of Tables 6 and 4 indicates that the algorithm performed better in the Tulsa, Oklahoma case. However, significant difference was noted only for the air temperature variable, for which the errors doubled in Lewistown, Montana.

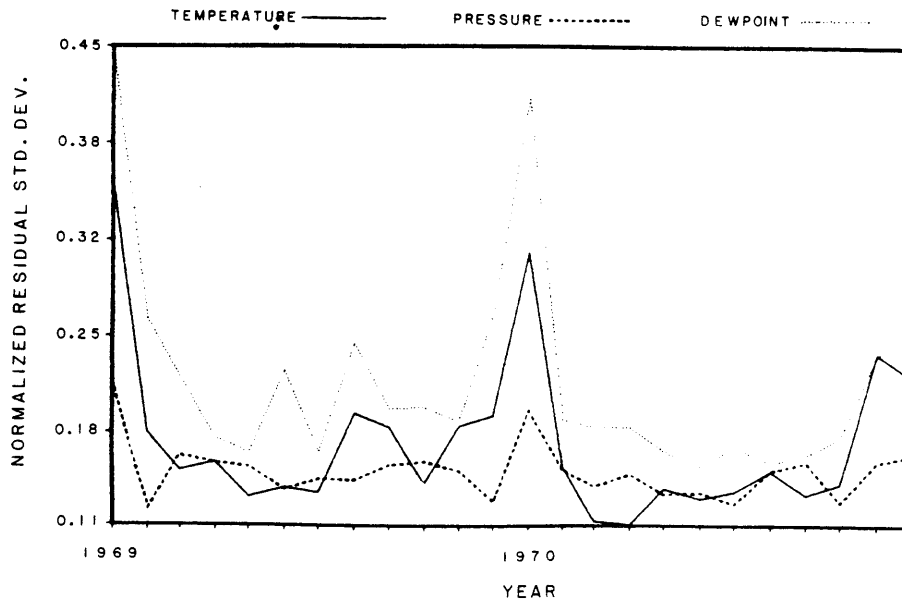


Fig. 12. Residual monthly standard deviations normalized by total record observations standard deviations for Lewistown, Montana. Both the topography component and the atmospheric disturbances component were used in the interpolation.

TABLE 5. Total Record Statistics for Lewistown, Montana

Variable	Mean	Standard Deviation
Temperature	278.40, °K	12.03, °K
Pressure	87,186, kg/(m/s ²)	631, kg/(m/s ²)
Dew-point temperature	270.44, °K	8.85, °K

Note that discretization in vertical layers would improve the topography components in this case. Overall, judging from the statistics in Tables 4 and 6, the interpolation algorithm showed satisfactory performance in both cases.

SUMMARY

A three-component mathematical model has been formulated to simulate the rainfall-runoff process. Its first component describes the precipitation mechanism based on simplified cloud dynamics and microphysics. The second component is a spatially lumped representation of the soil moisture related processes. A nonlinear channel routing model constitutes the third component.

The model links together meteorological and hydrological concepts and data, for the purpose of forecasting river flows from headwater areas. The model equations are in state-space form suitable to be used with modern estimation theory techniques for real-time state updating from observations of mean areal precipitation and discharge.

The spatial interpolation problem related to the input variables temperature, pressure, and dew-point temperature was solved in two steps. First, the component of the variables that is due to the topographic relief was determined, using concepts from thermodynamics and air parcel ascent. Then, the component due to the spatial correlation of the variables resulting from the organization of atmospheric disturbances was obtained, based on simple linear interpolation concepts.

The product of the above effort is a stochastic conceptual hydrometeorological model that uses as input, exclusively, operationally forecast variables and produces, in real time, forecasts of basin mean areal precipitation and streamflow. The fact that the model integrates, in real time, information from meteorological and hydrological processes, thus reducing considerably the communication time between meteorological and hydrological forecasting operations, makes it particularly useful in real-time, flash-flood forecasting. In cases of large river systems with several tributary basins, where the number of model states (and consequently of computations) increases dramatically, the integrated nature of the hydrometeorological model leads to computationally efficient dynamic decomposition schemes [Georgakakos, 1983].

TABLE 6. Total Record Residual Standard Deviations for Lewistown, Montana

Variable	Standard Deviation
Temperature	2.1, °K
Pressure	97, kg/(m/s ²)
Dew-point temperature	1.9, °K

APPENDIX A: HEADWATER BASIN HYDROMETEOROLOGICAL MODEL SYMBOLS

Functions

- $f_p(t)$ Scalar function to represent the time derivative of the precipitation model state.
- $f_s(t)$ Vector function whose i th component represents the time derivative of the i th soil state.
- $f_c(t)$ Vector function whose i th component represents the time derivative of the i th storage element of the channel model.
- $h_p(t)$ Scalar function that gives the relationship between the precipitation rate observed and the hydro-meteorological model states.
- $h_c(t)$ Scalar function to represent the relationship between the discharge rate at the catchment outlet and the hydrometeorological model states.

States

- x_p Precipitation model state.
- x_s Vector of the soil model states.
- x_c Vector of channel states.

Input

- u Precipitation model input: T_0, p_0, T_d .
- u_e Potential evapotranspiration rate.

Parameters

- a_p Vector of precipitation model storm-invariant parameters.
- a_s Soil model parameters.
- a_c Channel-routing model parameters.

Output

- z_p Precipitation rate per unit area in the drainage basin.
- z_c Discharge rate at the drainage basin outlet.

APPENDIX B: PRECIPITATION MODEL CONSTANTS, INPUT VARIABLES, AND PARAMETERS

Constants

- ε 0.622.
- A 2.5×10^6 (J/kg).
- B 2.38×10^3 (J/(kg °K)).
- A_1 8×10^{-4} (kg/(m s² °K^{3.5})).
- A_2 2.11×10^{-5} (m² s).
- T^* 273.15 (°K).
- p^* 101325 (kg/(m s²)).
- p_n 10^5 (kg/(m s²)).
- g 9.80 (m/s²).
- R 287 (J/(kg °K)).
- R_i 461 (J/(kg °K)).
- c_p 1004 (J/(kg °K)).
- p 2×10^4 (kg/(m s²)).
- α 3500 (1/s) for rain; 1500 (1/s) for snow.
- c_1 7×10^5 (kg/(m³ s)) for rain; 1.4×10^5 (kg/(m³ s)) for snow.

Input (Vector u)

- T_0 Surface temperature.
- p_0 Surface pressure.
- T_d Surface dew-point temperature.

Parameters (Vector a_p)

ϵ_1	1.65×10^{-3} .
ϵ_2	5×10^4 (kg/(m s ²)).
ϵ_3	1 (s/m).
ϵ_4	5.5×10^{-5} (m).
γ	1.
β	1.
m	0.

Acknowledgments. This work was sponsored by the National Oceanic and Atmospheric Administration of the U.S. Department of Commerce, and by the U.S. National Research Council. The research work took place at the Hydrologic Research Laboratory of the National Weather Service, NOAA while the author was a National Research Council—NOAA Research Associate. The comments of R. L. Bras, M. D. Hudlow, E. A. Anderson, D. L. Fread, R. K. Farnsworth, W. F. Krajewski, and G. F. Smith are gratefully acknowledged. This document was benefited by the editorial comments of L. T. Iseley.

REFERENCES

- Armstrong, B. L., Derivation of initial soil moisture accounting parameters from soil properties for the National Weather Service river forecast system, *Rep. NWS HYDRO-37*, Natl. Oceanic and Atmos. Admin., Silver Spring, Md., 1978.
- Bras, R. L., and I. Rodriguez-Iturbe, *Random Functions and Hydrology*, Addison-Wesley, Reading, Mass., 1985.
- Burnash, R. J. C., R. L. Ferral, and R. A. McGuire, A generalized streamflow simulation system—Conceptual modeling for digital computers, technical report, 204 pp., Natl. Weather Serv., NOAA and State of Calif. Dep. of Water Resour., Joint Federal-State River Forecast Cent., Sacramento, Calif., 1973.
- Gelb, A., ed., *Applied Optimal Estimation*, The M.I.T. Press, Cambridge, Mass., 1974.
- Georgakakos, K. P., Structure and parameter determination of a hydrologically useful rainfall prediction model, paper presented at the 1982 Fall Meeting of the American Geophysical Union, AGU, San Francisco, Calif., 1982.
- Georgakakos, K. P., Stochastic decomposition schemes for the real-time forecasting of river flows in a large river system, *Hydro. Tech. Note 1*, Off. of Hydrol., NWS/NOAA, Silver Spring, Md., 1983.
- Georgakakos, K. P., Model-error adaptive parameter determination of a conceptual rainfall prediction model, paper presented at Proceedings of the 16th Southeastern Symposium on System Theory, Inst. of Elec. and Electron. Eng., Miss. State, Miss., March 25–27, 1984.
- Georgakakos, K. P., A generalized stochastic hydrometeorological model for flood and flash-flood forecasting, 2, Case studies, *Water Resources Research*, this issue.
- Georgakakos, K. P., and R. L. Bras, On-line river discharge forecasting using filtering and estimation theory, Progress report, Sept. 13, 1978–Feb. 13, 1979, Ralph M. Parsons Lab., Dep. of Civ. Eng., M.I.T., Cambridge, Mass., 1979.
- Georgakakos, K. P., and R. L. Bras, A statistical linearization approach to real-time nonlinear flood routing, *Rep. TR 235*, Ralph M. Parsons Lab., Dep. of Civ. Eng., M.I.T., Cambridge, Mass., 1980.
- Georgakakos, K. P., and R. L. Bras, A precipitation model and its use in real-time river flow forecasting, *Rep. TR 286*, Ralph M. Parsons Lab., Hydrol. and Water Resour. Sys., Dep. of Civ. Eng., M.I.T., Cambridge, Mass., 1982a.
- Georgakakos, K. P., and R. L. Bras, Real-time, statistically linearized adaptive flood routing, *Water Resour. Res.*, 18(3), 513–524, 1982b.
- Georgakakos, K. P., and R. L. Bras, A hydrologically useful station precipitation model. 1, Formulation, *Water Resour. Res.*, 20(11), 1585–1596, 1984a.
- Georgakakos, K. P., and R. L. Bras, A hydrologically useful station precipitation model. 2, Case studies, *Water Resour. Res.*, 20(11), 1597–1610, 1984b.
- Georgakakos, K. P., and M. D. Hudlow, Quantitative precipitation forecast techniques for use in hydrologic forecasting, *Bull. Am. Meteorol. Soc.*, 65(11), 1186–1200, 1984.
- Georgakakos, K. P., P. J. Restrepo-Posada, and R. L. Bras, On-line river discharge forecasting using filtering and estimation theory, Progress report, Aug. 13, 1979–Jan. 13, 1980, Ralph M. Parsons Lab., Dep. of Civ. Eng., M.I.T., Cambridge, Mass., 1980.
- Kitanidis, P. K., and R. L. Bras, Real-time forecasting with a conceptual hydrologic model. 1, Analysis of uncertainty, *Water Resour. Res.*, 16(6), 1025–1033, 1980a.
- Kitanidis, P. K., and R. L. Bras, Real-time forecasting with a conceptual hydrological model. 2, Applications and results, *Water Resour. Res.*, 16(6), 1034–1044, 1980b.
- Peck, E. L., Catchment modeling and initial parameter estimation for the National Weather Service river forecast system, *Rep. NWS HYDRO-31*, Natl. Oceanic and Atmos. Admin., Silver Spring, Md., 1976.
- Puente Angulo, C. E., and R. L. Bras, Nonlinear filtering, parameter estimation and decomposition of large rainfall-runoff models, *TR 297*, Ralph M. Parsons Lab., Hydrol. and Water Resour. Sys., Dep. of Civ. Eng., M.I.T., Cambridge, Mass., 1984.
- Restrepo-Posada, P. J., and R. L. Bras, Automatic parameter estimation of a large conceptual rainfall-runoff model: A maximum likelihood approach, *TR 267*, Ralph M. Parsons Lab., Dep. of Civ. Eng., M.I.T., Cambridge, Mass., 1982.
- Ripley, B. D., *Spatial Statistics*, John Wiley, New York, 1981.
- Analytic Sciences Corporation, TASC, Applications of Kalman filtering and maximum likelihood parameter identification to hydrologic forecasting, *Rep. TR-1480-1*, Reading, Mass., 1980.
- Wallace, J. M., and P. V. Hobbs, *Atmospheric Science, An Introductory Survey*, Academic, Orlando, Fla., 1977.

K. P. Georgakakos, Department of Civil and Environmental Engineering, Iowa Institute and Hydraulic Research, The University of Iowa, Iowa City, IA 52242.

(Received December 6, 1985;

revised July 10, 1986;

accepted July 31, 1986.)

